Impact of Storm Size on Prediction of Storm Track and Intensity Using the 2016 Operational GFDL Hurricane Model

MORRIS A. BENDER

Program in Atmospheric and Oceanic Sciences, Princeton University, Princeton, New Jersey

TIMOTHY P. MARCHOK

NOAA/GFDL, Princeton, New Jersey

CHARLES R. SAMPSON

Naval Research Laboratory, Monterey, California

JOHN A. KNAFF

NOAA/Center for Satellite Applications and Research, Fort Collins, Colorado

MATTHEW J. MORIN

Engility Holdings, Inc., Chantilly, Virginia

(Manuscript received 20 December 2016, in final form 12 May 2017)

ABSTRACT

The impact of storm size on the forecast of tropical cyclone storm track and intensity is investigated using the 2016 version of the operational GFDL hurricane model. Evaluation was made for 1529 forecasts in the Atlantic, eastern Pacific, and western North Pacific basins, during the 2014 and 2015 seasons. The track and intensity errors were computed from forecasts in which the 34-kt (where 1 kt = 0.514 m s^{-1}) wind radii obtained from the operational TC vitals that are used to initialize TCs in the GFDL model were replaced with wind radii estimates derived using an equally weighted average of six objective estimates. It was found that modifying the radius of 34-kt winds had a significant positive impact on the intensity forecasts in the 1–2 day lead times. For example, at 48 h, the intensity error was reduced 10%, 5%, and 4% in the Atlantic, eastern Pacific, and western North Pacific, respectively. The largest improvements in intensity forecasts were for those tropical cyclones undergoing rapid intensification, with a maximum error reduction in the 1–2 day forecast lead time of 14% and 17% in the eastern and western North Pacific, respectively. The large negative intensity biases in the eastern and western North Pacific were also reduced 25% and 75% in the 12–72-h forecast lead times. Although the overall impact on the average track error was neutral, forecasts of recurving storms were improved and tracks of nonrecurving storms degraded. Results also suggest that objective specification of storm size may impact intensity forecasts in other high-resolution numerical models, particularly for tropical cyclones entering a rapid intensification phase.

1. Introduction

The National Hurricane Center (NHC), Central Pacific Hurricane Center (CPHC), and Joint Typhoon Warning Center (JTWC), provide 6-hourly forecasts of tropical cyclone (TC) tracks, intensities, and surface wind structures for all active TCs worldwide. The initial and forecast TC wind structures are provided in terms of the maximum extent of the gale [34 knots (kt), where 1 kt = 0.514 m s^{-1}], 50-kt, and hurricane (64 kt) force winds in four quadrants surrounding the TC (i.e., northeast, southeast, southwest, and northwest quadrants). These are collectively referred to as wind radii and estimating them is a critical part of the forecast process. The JTWC area of responsibility includes the

Corresponding author: Morris A. Bender, morris.bender@noaa.gov

DOI: 10.1175/WAF-D-16-0220.1

western North Pacific, northern Indian Ocean, and the entire Southern Hemisphere, while the NHC is responsible for TCs in the Atlantic and eastern North Pacific east of 140°W. Finally, the CPHC is responsible for TCs in the Northern Hemisphere between 140°W and the international date line. For the remainder of the paper the authors will use "east Pacific" to refer to the eastern North Pacific and "west Pacific" to refer to the western North Pacific. Wind speed results are reported in knots and distances are reported in nautical miles (n mi; 1 n mi = 1.852 km), as those are the units used in U.S. operations.

As discussed in Sampson et al. (2017), each U.S. forecast center uses its own techniques and methodologies to estimate the TC wind radii that are used as input for operational numerical weather prediction (NWP) models. This information and other key observations of the TC (maximum wind and radius, central pressure, storm location, and pressure and radius of the outermost closed isobar) are summarized in a unique message file called the TC vitals, which is prepared every 6 h by these forecasting centers. In most cases wind radii estimates made by operational centers are based on subjective analyses of available information. In situ observations such as surface reports and buoy observations can provide high quality ground truth, but these observations are not routinely available. Aircraft reconnaissance can also provide a detailed spatial distribution of the low-level or surface winds, but these are rarely available outside the North Atlantic region. The dearth of in situ observations makes routine operational wind radii estimation heavily dependent upon satellite observations and satellite-derived techniques. Satellite observations include cloud/feature-tracked winds (Holmlund et al. 2001; Velden et al. 2005), scatterometry (Jones et al. 1975), and blended surface wind analyses (Knaff et al. 2011). Scatterometry has the ability to provide the best picture of the 34-kt wind field, but the data are intermittent and often only sample a part of a TC. In addition to these remotely sensed wind vectors, there are several estimates available to operations specifically designed to estimate TC vortex structure. These include techniques that estimate wind radii directly from microwave sounders (Demuth et al. 2004, 2006) and from information derived from infrared (IR) satellite imagery, TC intensity, and TC motion (Knaff et al. 2016). Each of these methods and observations has its own strengths, but also its own weaknesses. As a result, errors in operational wind radii estimates can be as large as 25%–40% of the radii themselves (see Knaff and Harper 2010; Knaff and Sampson 2015; Landsea and Franklin 2013) with uncertainties on the order of 25 n mi (Sampson et al. 2017).

Nonetheless, the production of quality wind radii is important to operations for a number of reasons. The TC vitals files provide initial conditions for a number of applications such as wind speed probabilities (DeMaria et al. 2009, 2013), TC conditions of readiness (Sampson et al. 2012), and sea surface wave forecasting (Sampson et al. 2010). The TC vitals wind radii, intensity, position, and other structural characteristics are also the primary input from the TC forecast centers to numerical models like the Geophysical Fluid Dynamics Laboratory's hurricane model (GFDL; Kurihara et al. 1993; Bender et al. 2007, 2016) and the Hurricane Weather Research and Forecasting Model (HWRF; Tallapragada et al. 2014) for vortex specification and initialization purposes. This information is provided near the beginning of TC forecast cycles, which begin at 0000, 0600, 1200, and 1800 UTC at U.S. TC forecast centers. It is this latter application that will be the focus of this paper.

In the few studies that exist in the literature, the quality of the wind radii estimates provided in the TC vitals has been found to have an impact on TC-focused NWP forecasts. For example, Kunii (2015) found that the inclusion of wind radii data helped improve TC track forecasts in the Japan Meteorological Agency's (JMA) operational mesoscale model. Also, Marchok et al. (2012) showed that modifying the observed 34- and 50-kt wind radii used to initialize the GFDL hurricane model had an impact on intensity forecasts by modifying the bias. And finally, Wu et al. (2010) found significantly improved evolution of TC structure in the Weather Research and Forecasting Model during vortex initialization by assimilating wind radii information using an ensemble Kalman filter. Montgomery and Smith (2014) pointed out that as a vortex intensifies and contracts, the maximum tangential wind should tend to increase as angular momentum is conserved. This would suggest that a proper specification of the TC initial storm size and angular momentum distribution could impact the storm intensification process as the vortex spins up. However, large and comprehensive sensitivity studies of the effects of wind radii variations on NWP forecasts have yet to be undertaken.

The purpose of this paper is to provide such a study, by investigating the impacts of wind radii initial conditions from two sources on forecasts made by the GFDL forecast system. The first source of wind radii information is the TC vitals provided operationally by NHC and JTWC. The second source is an objective best-track technique (OBTK; Sampson et al. 2017) that provides estimates of gale force wind radii from a combination of satellite and short-term model forecasts. The OBTK has been implemented in the Automated Tropical Cyclone Forecast System (ATCF; Sampson and Schrader 2000) and has been available to JTWC since September 2016 as guidance for real-time

estimates of the wind radii. This study will test the OBTK impacts on NWP guidance using two years (2014–15) of TC forecasts from three tropical cyclone basins (North Atlantic, east Pacific, and west Pacific). Details of the methods, model setup, results, and implications are discussed in the following sections.

2. Methodology

a. The GFDL model

The regional, triply nested GFDL hurricane model has been operational since 1995 for the National Weather Service (NWS) and since 1996 for the U.S. Navy, providing numerical guidance on tropical cyclone track, intensity, and surface wind structure for forecasters at NHC, CPHC, and JTWC. The National Centers for Environmental Prediction's (NCEP) Global Forecast System (GFS) analysis serves as the initial background field for the operational GFDL hurricane model run by the NWS, and the U.S. Navy's Global Environmental Model (NAVGEM: Hogan et al. 2014) provides the analysis used for the navy's version of the GFDL forecast system (GFDN). A critical part of the GFDL operational forecast system is the initialization step in which the vortex resolved in the global analysis is replaced with a specified vortex that is designed to accurately represent the initial observed storm structure. In the GFDL vortex initialization scheme detailed in Kurihara et al. (1993, 1995) and still in use in the GFDL forecast system, a filtering technique is employed to remove the tropical cyclone vortex in the global model fields and replace it with a more realistic and model-consistent vortex. In the GFDL methodology, the specified vortex is generated by a vortex spinup technique in which an axisymmetric version of the 3D hurricane model with identical physics and resolution of the innermost nest ($1/18^\circ$) of the full 3D model is integrated for 60 h. This technique was developed to enable the initial vortex at the start of the GFDL forecast to be more consistent with the hurricane model physics and resolution, creating a storm structure that better matches that of the observed TC. In the axisymmetric vortex spinup process, the tangential winds in the free atmosphere are gradually nudged toward a target storm wind profile. The target wind profile is determined by the observed maximum wind and its radius, the central pressure, and the 50-kt (if available) and 34-kt (gale force) wind radii provided in the TC vitals file. Four wind profiles, one for each of the wind radii quadrants, are averaged to produce the appropriate target tangential wind profile for the axisymmetric integration. In the GFDL model approach, the other prognostic variables including moisture are not forced, but are free to evolve in a model-consistent way during the 60-h axisymmetric model integration. At the completion of this step, the wind, mass, and moisture fields are interpolated to create a 3D vortex, which is then inserted back into the GFS environmental fields (global analysis minus the global vortex) at the initial storm location. Using this technique both the central pressure and maximum surface winds match well with the observed values from the TC vitals at hour 0. However, for intense storms, particularly those with very small radii of maximum winds that are not well resolved by the finest mesh resolution ($1/18^\circ$), some reduction in the maximum winds occurs after the start of the integration, with readjustment of the wind field within the first few hours.

An important variable used in the specification of the target wind profile for the vortex spinup is the radial extent of the specified vortex R_b, defined as the point where the tangential wind in the target profile goes to zero. Prior to 2015, R_b was defined in the GFDL initialization as 1.5 times the radius of the outermost closed isobar, obtained from the operational TC vitals file. In 2015, a new specification for R_b was derived based on the formulation introduced by Carr and Elsberry (1997), which modeled the storm tangential wind in the outer regions of a TC based on angular momentum conservation principles for a parcel moving radially inward from R_b to the storm center.

To obtain R_b, the angular momentum M at the average 34-kt (gale force) radius in the GFDL target profile is defined as

$$M_{\text{gale}} = r_{\text{gale}} v_{\text{gale}} + \frac{1}{2} f r_{\text{gale}}^2 , \tag{1}$$

where v_{gale} is the tangential wind at the average 34-kt (gale force) radius r_{gale}. After algebraic manipulation, a new estimate for R_b is obtained:

$$R_b = e^{[\text{MLG}/(1+x)]} , \tag{2}$$

where $x = 0.4$ and MLG in Eq. (2) is defined as

$$\text{MLG} = \log(2M_{\text{gale}}/f r_{\text{gale}}^{(1-x)}) . \tag{3}$$

Note that by using this new formulation, the storm tangential wind profile in the GFDL initialization is more strongly dependent on a reasonable specification of the gale force wind radii. Hence, an accurate estimation of the gale force wind radii is essential for the initialization to accurately depict the correct storm size (i.e., R_b) and structure. Sampson et al. (2017) demonstrated that the GFDL technique provided a reasonable initial storm structure, with initial gale force wind radii

errors and biases that are comparable to those from other operational models (e.g., HWRF or GFS).

In the original operational initialization system introduced in 1995, an asymmetric component was computed through integration of a barotropic vorticity equation (Kurihara et al. 1993) and inserted at initialization along with the symmetric component. In 1998, this beta gyre asymmetry (cf. Fiorino and Elsberry 1989) was replaced by a technique developed to estimate hurricane vortex asymmetries obtained from the previous 12-h forecast (Bender et al. 2007). The addition of any asymmetric component was removed from the initialization procedure in the 2008 upgrade after a multiyear evaluation showed it no longer contributed to improved hurricane track or intensity prediction in any of the forecast lead times. Thus, in the version of the initialization used in this current study, the OBTK only impacted the initialization and forecast through the symmetric component. It is possible that use of the OBTK could have had more of a track forecast impact if an asymmetric component was used as part of the initialization.

b. *The OBTK estimates*

The OBTK estimates are an equally weighted average of as many as six independent estimates of the gale force wind radii. These estimates include the GFS, HWRF, and GFDL model 6-h forecasts from the previous model cycle (the analyses from the current cycle are not available in real time), operational estimates from the microwave sounder method described in Demuth et al. (2006), Dvorak-based estimates described in Knaff et al. (2016), and the operational multiplatform estimates from the method described in Knaff et al. (2011). A 6-h sampling window is employed to capture and use the most recent observations and allows for some latency in the observations. When applied, the OBTK gale force wind radii estimates were found to have mean errors and biases comparable to or better than those from the individual best-performing members (Sampson et al. 2017) and the averaging also helps to provide some temporal stability in these estimates. As discussed in section 1, OBTK estimates are now being produced in real time at JTWC, where these estimates provide realistic gale force wind radii, even in the absence of aircraft data, conventional observations, and scatterometry.

While the OBTK generates adequate gale wind radii estimates for forecasters, little is known about its potential impact on NWP. The operational GFDL hurricane model, which has been run operationally for two decades across all the world's basins (Bender et al. 2007), and which requires limited computer resources, is an ideal choice to provide a rigorous evaluation of the OBTK's potential impact on NWP through the examination of intensity and track forecasts.

c. *Presentation of results*

Results analyzed in this study are based on the combined 2014 and 2015 tropical cyclone seasons in the west Pacific, Atlantic, and east Pacific basins. The focus on this 2-yr sample was motivated by the availability of initial and forecast fields for the 2016 version of the GFS for the summer months of 2014 and 2015, from 1 July through 30 November. Although several gaps in GFS availability occurred in 2014, the vast majority of forecast time periods were available, enabling a large sample of 603, 280, and 646 forecasts to be used in the west Pacific, Atlantic, and east Pacific, respectively. To enable this evaluation to be as objective as possible, a forecast was initiated for all four synoptic times in these three basins during the complete life cycle of every tropical cyclone during the 1 July–30 November time period (assuming the availability of the GFS data). Five-day forecasts were first made with the operational TC vitals information (the control), and then from an experimental group using the identical system but replacing the gale force wind radii at each quadrant with the values obtained by the OBTK. Since the gale force wind radii are available more often, are most easily observed and estimated using the OBTK method, and to keep this experiment relatively simple, the differences in initialization between the control and experimental groups are based solely on the gale force wind radii differences between the TC vitals and the OBTK (i.e., the 50- and 64-kt radii from the operational TC vitals file were ignored). This large sample also captured a wide range of tropical cyclone categories, sizes, and structures that occurred in the Northern Hemisphere, and ensured a large enough sample from which to draw statistically solid conclusions.

3. Results

a. *Comparison of wind radii*

For the combined 2-yr dataset, Table 1 compares the estimates of the average gale force wind radii for storms in each of the three basins from both the operational TC vitals and the OBTK. Note that the largest differences between the two methods were in the west Pacific, where the average OBTK gale radii were 27% larger than the operational TC vitals gale radii. These differences reinforce the need for accurate and timely TC structure estimates to be available to the forecaster, especially given the time window (30–60 min) available for the TC vitals to be created. This is particularly true at JTWC where a typhoon duty officer (TDO) may be forecasting for several storms at once and may not have timely observations to specify changes in the gale force wind radii. Since the OBTK wind radii are based mostly

TABLE 1. Comparison of the average gale force wind radii, obtained from the operational TC vitals and the OBTK (italics) in the four quadrants surrounding the storms (northeast, southeast, southwest, and northwest), and including the average of the four quadrants. Percentage change for the average of the OBTK over the operational TC vitals radii is also indicated.

Atlantic basin					
NE	SE	SW	NW	Avg radii	
102	111	91	72	94	Operational TC vitals radii (n mi)
102	*109*	*93*	*80*	*96*	*OBTK radii (n mi)*
Avg difference					+2%
East Pacific basin					
NE	SE	SW	NW	Avg radii	
95	89	69	69	81	Operational TC vitals radii (n mi)
100	*90*	*74*	*89*	*88*	*OBTK radii (n mi)*
Avg difference					+8%
West Pacific basin					
NE	SE	SW	NW	Avg radii	
127	124	120	122	123	Operational TC vitals radii (n mi)
171	*162*	*138*	*150*	*156*	*OBTK radii (n mi)*
Avg difference					+27%

on short-term NWP forecasts and satellite data proxies, a radii expansion can be identified earlier (e.g., Table 1).

The initialization method outlined in section 2 produced initial distributions of the 10-m winds that retained those differences between the operational TC vitals and the OBTK input data. For example, the average differences in the west Pacific gale force wind radii between both initialization methods was 23% at hour 0 (Fig. 1) for all cases, as compared with a difference of 27% in the radii taken directly from the TC vitals input datasets. During the 1–5-day forecast period the differences in the radii decreased in the west Pacific, but in all three basins the forecasts initialized with OBTK gale radii remained larger than the forecasts initialized with the operational TC vitals (Fig. 1).

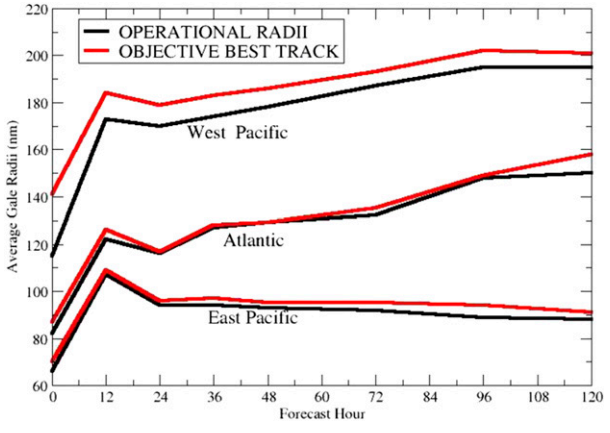

FIG. 1. Comparison of the average gale force (34 kt) wind radii estimates computed from the 10-m wind fields vs forecast lead time for the forecasts initialized from the operational TC vitals (black) and the OBTK (red) for the west Pacific, Atlantic, and east Pacific basins.

Three examples of large differences in the radii estimates occurring with west Pacific Typhoons Soudelor, Neoguri, and Nuri are shown in Table 2. In the Atlantic and east Pacific, the differences were typically smaller than in the west Pacific, and the average OBTK gale radii were only 2% and 8% larger than the operational TC vitals, respectively. However, an examination of individual cases in these two basins revealed some cases with significantly larger bias with the OBTK, such as the initial radii estimates of Hurricane Joaquin at 1200 UTC 29 September 2015 (Table 2). The large differences between the OBTK and the operational TC vitals demonstrate how the availability of the data in real time can impact these estimates.

TABLE 2. Comparison of the gale force wind radii, obtained from the operational TC vitals and the OBTK (italics) in the four quadrants surrounding the storms (northeast, southeast, southwest, and northwest), for Typhoon Soudelor (13W), Hurricane Joaquin (11L), Typhoon Neoguri (08W), and Typhoon Nuri (20W).

Typhoon Soudelor (13W)				0600 UTC 2 Aug 2015
NE	SE	SW	NW	
75	35	35	80	Operational TC vitals radii (n mi)
150	*95*	*75*	*135*	*OBTK radii (n mi)*
Hurricane Joaquin (11L)				1200 UTC 29 Sep 2015
NE	SE	SW	NW	
0	60	0	0	Operational TC vitals radii (n mi)
70	*130*	*90*	*70*	*OBTK radii (n mi)*
Typhoon Neoguri (08W)				0000 UTC 4 Jul 2014
NE	SE	SW	NW	
30	30	25	25	Operational TC vitals radii (n mi)
140	*155*	*150*	*110*	*OBTK radii (n mi)*
Typhoon Nuri (20W)				0060 UTC 1 Nov 2014
NE	SE	SW	NW	
65	55	55	60	Operational TC vitals radii (n mi)
125	*110*	*90*	*105*	*OBTK radii (n mi)*

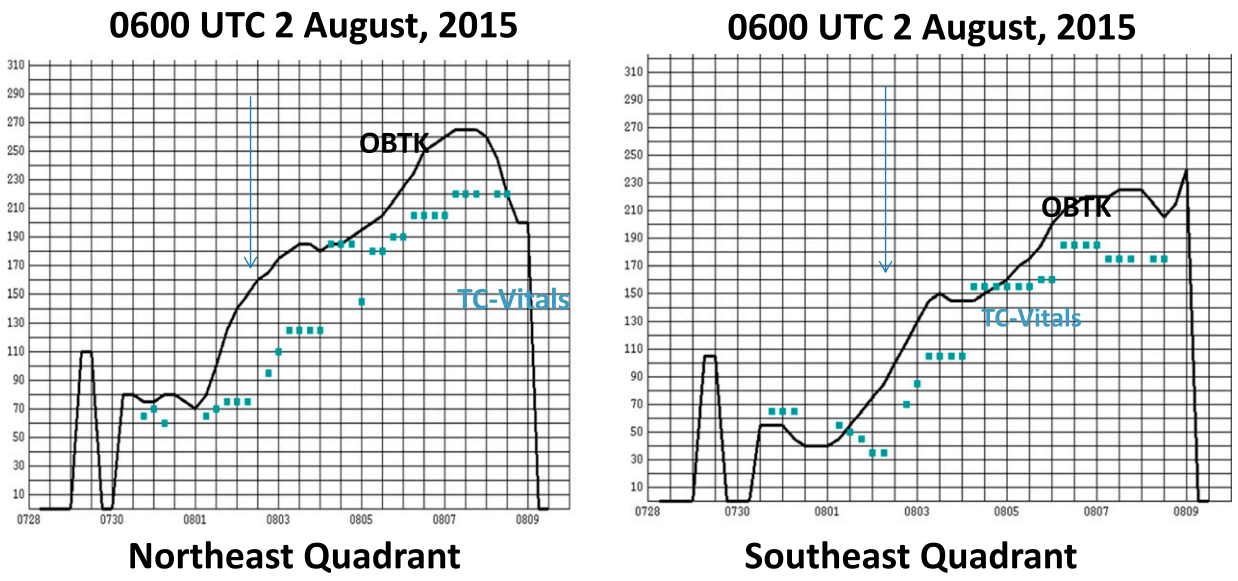

FIG. 2. Plots of gale force (34 kt) wind radii estimates vs time for the entire life cycle of Typhoon Soudelor (13W) for the OBTK (black line), and the operational TC vitals (blue squares) for the northeast and southeast quadrants surrounding the storm. The 0600 UTC 2 Aug 2015 synoptic time used to initialize the forecast presented in Fig. 3 (top) is identified by the vertical blue arrows.

Sampson et al. (2017) also showed that the average gale force wind radii using the OBTK are consistently larger than the operational TC vitals in the west Pacific compared with the Atlantic and east Pacific. Figure 2 shows a comparison between the operational estimates of the gale force wind radii from the TC vitals and the OBTK for the entire life cycle of Typhoon Soudelor (13W). The operational gale radii appear to "stair step" with time, reflecting the availability of new information (e.g., a scatterometer pass), while the OBTK provides a smooth rendition of the growth and decay of the gale radii. Using the GFDL initialization with the operational TC vitals and the OBTK, the initial 10-m wind distributions in the inner nest are shown (Fig. 3) for Typhoon Soudelor (0600 UTC 2 August 2015) and Hurricane Joaquin (1200 UTC 29 September 2015) just before the onset of rapid intensification (RI), as shown in the left panels of Fig. 4.

b. *Impact on track and intensity*

Despite the large differences in the initial storm structure, the overall impact on track was relatively small for these two forecasts (Fig. 5), although the track forecast of Joaquin was somewhat improved after day 3 in the OBTK experiment. On the other hand, a much more significant impact was found in the experimental intensity prediction for Soudelor and Joaquin (Fig. 4, left panels), with nearly a 35-kt reduction in forecast error in both cases near the time of maximum intensity. The most significant impact on intensity was the model's improved ability to forecast RI with the larger and more temporally smooth OBTK gale wind radii. For example, nearly constant intensity through 1- and 3-day lead times was predicted by the GFDL model for Hurricane Joaquin using the operational wind radii estimates, while steady intensification to major hurricane status (maximum winds > 95 kt) in 3 days was predicted using the OBTK, which was a closer match to the observed rapid intensification. A similar impact was found in the prediction of RI for two other typhoons during the 2014 west Pacific season (Fig. 4, right panels): Typhoon Neoguri (08W) and Typhoon Nuri (20W). Note that in all four of these cases where the gale radii specified by the OBTK were larger than the operational TC vitals, the prediction of RI was improved in the OBTK experiment.

Numerous studies (e.g., Anthes and Hoke 1975; Madala and Piacsek 1975; DeMaria 1985; Holland 1984) have confirmed that the advection of earth vorticity by an axisymmetric vortex will induce storm motion, typically referred to as the beta drift, with the translational speed averaging about $2\,\mathrm{m\,s^{-1}}$ in a general direction varying from northwest to north. The beta drift however can be significantly impacted by the distribution of the tangential wind in the outer storm regions with little sensitivity to the wind distribution in the storm core (DeMaria 1985; Holland 1984). DeMaria (1985) pointed out that the sensitivity of the storm track to the vortex structure can be less significant when the environmental absolute vorticity gradient is small. Consequently, the impact of the beta drift remains difficult to evaluate in

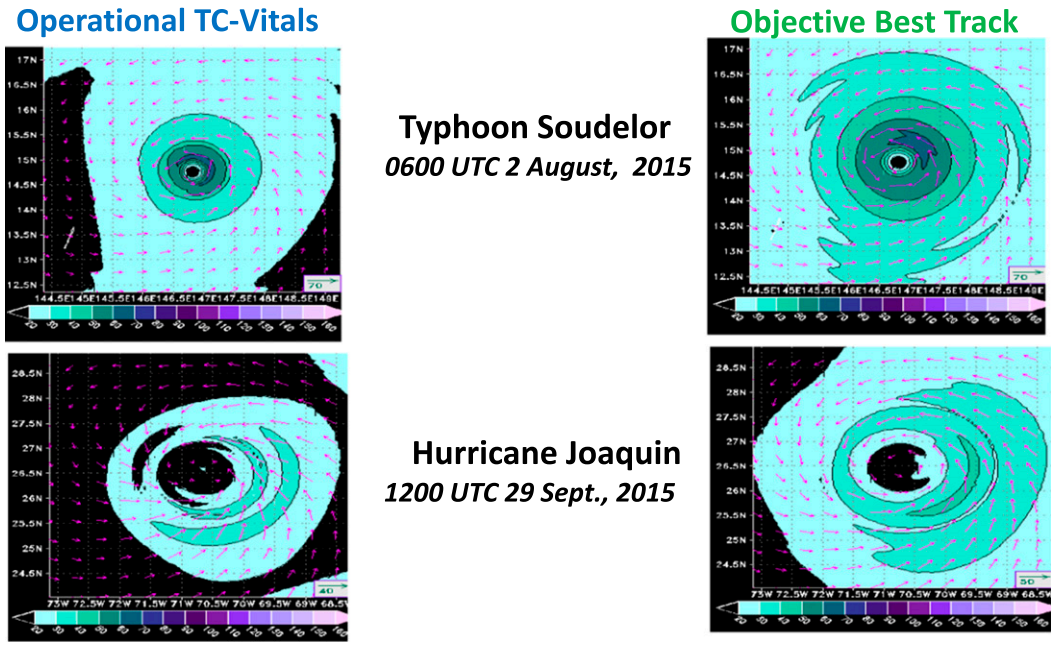

FIG. 3. Initial distribution of the 10-m winds [magnitude (shaded) and barbs; kt] for the innermost nest, for the forecasts of (top) Typhoon Soudelor initialized at 0600 UTC 2 Aug 2015 and (bottom) Hurricane Joaquin initialized at 1200 UTC 29 Sep 2015, using (left) the gale radii from the operational TC vitals and (right) the OBTK.

real case studies where complex interactions with the environmental flow exist and, as outlined below, the beta drift is masked by other more important impacts on the track.

An evaluation of the average track errors was conducted for all cases in the Atlantic and east and west Pacific basins for both the control and the OBTK experiments. The impact on the average track forecast error was found to be neutral in the three basins and at virtually all lead times (Fig. 6) with the OBTK experiment having improved tracks at 2–5 days for only 51% of the cases. However, further examination of the individual cases indicated that large track differences occurred in some storms. Two examples are shown (Fig. 7, bottom panels) along with the comparison of the axisymmetric tangential wind profile used (top panels), for a westward-moving storm (Typhoon Dujuan, left panels) and a recurving system (Typhoon Neoguri). In both of these examples, the OBTK-based gale radii were significantly larger (32% and 45%, respectively), so some influences of size-induced changes in the beta drift could be expected. Holland (1984) pointed out that recurving TCs may be particularly sensitive to the small changes in storm motion induced by changes in the storm structure. Most of the tracks of Neoguri were significantly improved with the OBTK, particularly just before and during the time of recurvature, and the average 5-day track error decreased nearly 25%. In contrast, the tracks of Typhoon Dujuan were degraded by 33% with the use of the OBTK radii. The control forecasts of Dujuan consistently predicted a much weaker storm (e.g., 20 kt weaker at 48 h for the 1800 UTC 24 September 2015 case) with a shallower system, which likely contributed to the more westward track as a shallower and weaker system will typically move faster under the influence of the subtropical ridge.

To better isolate the impacts of the OBTK on track, a list was compiled of TCs with the largest track changes, using a criterion of differences in average 5-day track error in excess of 10% (Table 3). Eight TCs in this sample had average 5-day track errors that were worse when using OBTK radii (ranging from 11% to 33%), while seven TCs demonstrated decreased 5-day error (from −12% to −34%). Despite the large impact on individual TCs, the average change in forecast error at day 5 for the 15 cases was only 0.2%. As summarized in Table 3, seven of the eight TCs with larger 5-day track errors were nonrecurving while only one (Typhoon Krovanh, 2015) was a recurving TC. Of the seven with improved tracks, five were recurving storms and only two were nonrecurving.

For the nonrecurving, westward-moving TCs in Table 3, the tracks for the 214 forecasts with the operational TC vitals exhibited a slight easterly bias (40 n mi at day 5). The negative intensity bias was 2–3 times larger at all forecast lead times compared with the OBTK experiment.

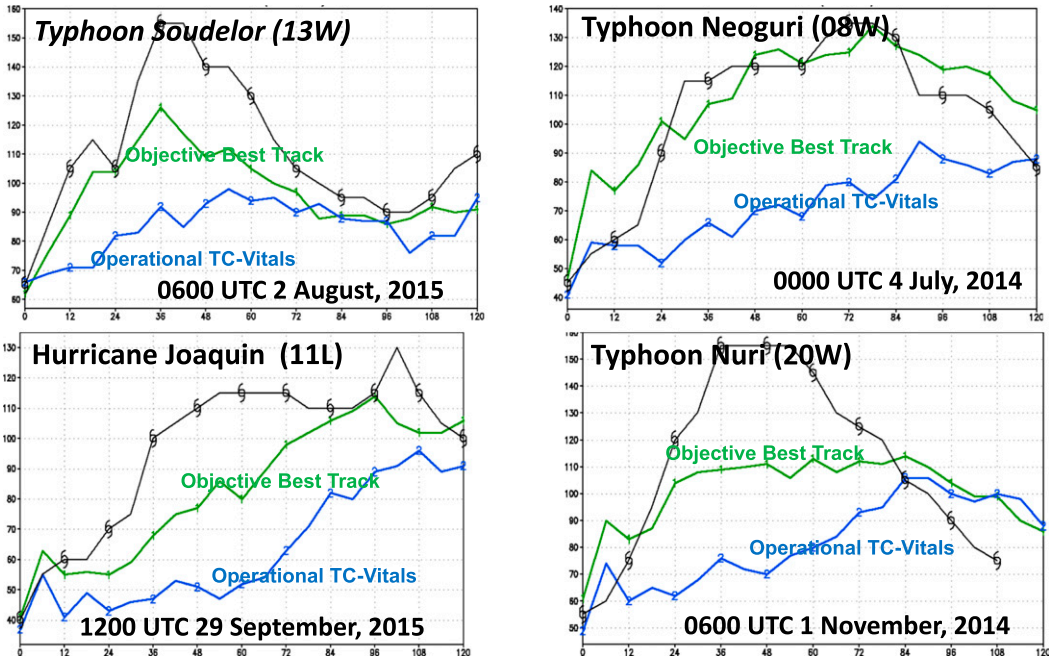

FIG. 4. Forecasts of maximum surface winds (kt) using gale radii from the operational TC vitals (blue) and the OBTK (green), for (top left) Typhoon Soudelor (13W) initialized at 0600 UTC 2 Aug 2015, (bottom left) Hurricane Joaquin (11L) initialized at 1200 UTC 29 Sep 2015, (top right) Typhoon Neoguri (08W) initialized at 0000 UTC 4 Jul 2014, and (bottom right) Typhoon Nuri (20W) initialized at 0600 UTC 1 Nov 2014. Observed intensity is indicated by the black line.

Similar to the Typhoon Dujuan case, the control experiment run with TC vitals forecasted weaker TCs that were likely under a greater influence of the easterlies to the south of the subtropical ridge. The deeper and stronger TCs produced using the OBTK wind radii exhibited a slow (east) bias at day 5 that was twice as large as the bias for the storms in the control experiment.

In contrast, the recurving storms that were initialized with the operational TC vitals exhibited a significant southerly bias (−110 n mi at day 5) and a 5-day error of 254 n mi mostly because recurvature was delayed. With the OBTK, the southerly bias was reduced by 30% and the 5-day track error decreased 13% as the prediction of recurvature was improved (Fig. 7, bottom-right panel). The recurving storms initialized with the OBTK had a much reduced negative intensity bias (i.e., 60% at 1–5-day forecast lead times), indicating stronger, more robust, and deeper circulations, which appear to have been steered sooner by the upper-level flow typically found at higher latitudes and thus captured into the westerlies. Since all of these storms were larger, an increased beta drift could also have contributed to more of a northerly component of motion. But separating the impact of these two effects is extremely difficult.

Results of an evaluation of the impact of OTBK gale force wind radii on the average intensity forecast errors for all three basins are shown in Fig. 8. Table 4 summaries these results and provides statistical significance, assuming a one-tailed Student's t test (Neumann et al. 1977), associated with the results. Although the impact on the average forecast track was small, the impact on intensity is substantially larger. In fact, the overall results in Fig. 8 and Table 4 show a clear reduction in average intensity forecast errors in the 1–3-day forecast lead times in all three basins. The largest improvements were in the 36–48-h forecast times, with a maximum improvement ranging from 7% in the west Pacific to 10% in the Atlantic and east Pacific (Table 4). These results are statistically significant (>95%) in all three basins at the critical 48-h forecast lead time, as well as also being statistically significant (>99%) in the east and west Pacific for 36-h forecasts.

Probability density functions (PDFs) for each of these basins for the combined 36- and 48-h forecast errors (Fig. 9, top panels) provide insight into where the OBTK gale wind radii had the greatest positive impact on the intensity errors. In all three basins, the greatest reduction of intensity errors using the OBTK initial conditions occurred when the control forecast significantly underpredicted intensity (negative intensity forecast bias). This result is consistent with the examples shown previously, where large negative forecast biases resulted

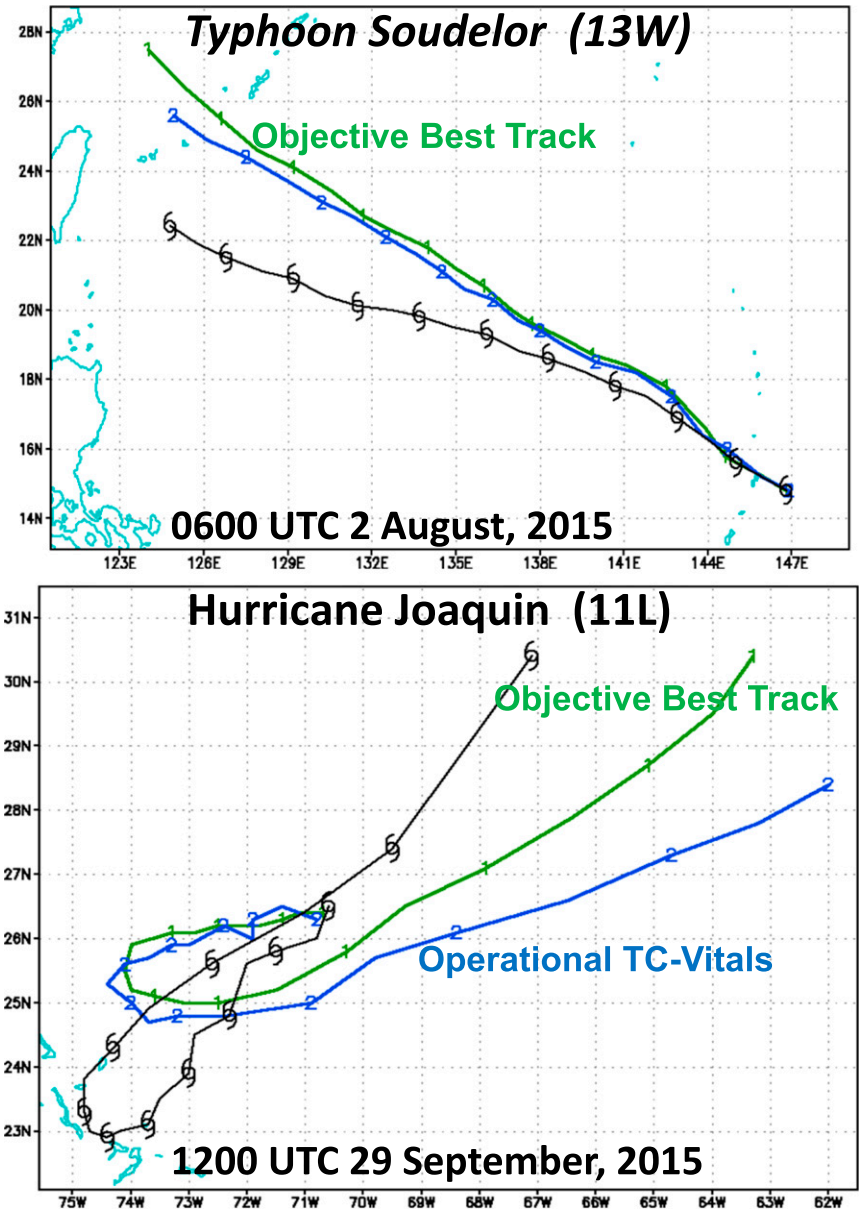

FIG. 5. Forecast storm tracks using gale wind radii from the operational TC vitals (blue) and the OBTK (green), for (top) Typhoon Soudelor (13W) initialized at 0600 UTC 2 Aug 2015 and (bottom) Hurricane Joaquin (11L) initialized at 1200 UTC 29 Sep 2015. Observed tracks are indicated by the black lines.

because of the model's failure to capture RI events when using radii from the operational TC vitals. The accumulated PDFs (Fig. 9, bottom panels) also show improved predictions of RI, particularly when the model underpredicted the RI by 20–80 kt. These improvements were slightly offset by a small increase in the magnitude of the positive intensity errors, suggesting a slightly increased positive intensity bias from forecasts using the OBTK initial conditions, particularly for the west Pacific.

For the 2014 and 2015 seasons, the Atlantic basin had only three storms that experienced RI events during their life cycles (e.g., Hurricanes Edouard and Gonzalo in 2014 and Hurricane Joaquin in 2015). On the other hand, a large majority of storms in the east and west Pacific basins during 2014 and 2015 underwent rapid intensification, using the standard criterion of 30 kt $(24\,\mathrm{h})^{-1}$ (Kaplan and DeMaria 2003), with many of these cases significantly exceeding this threshold. For

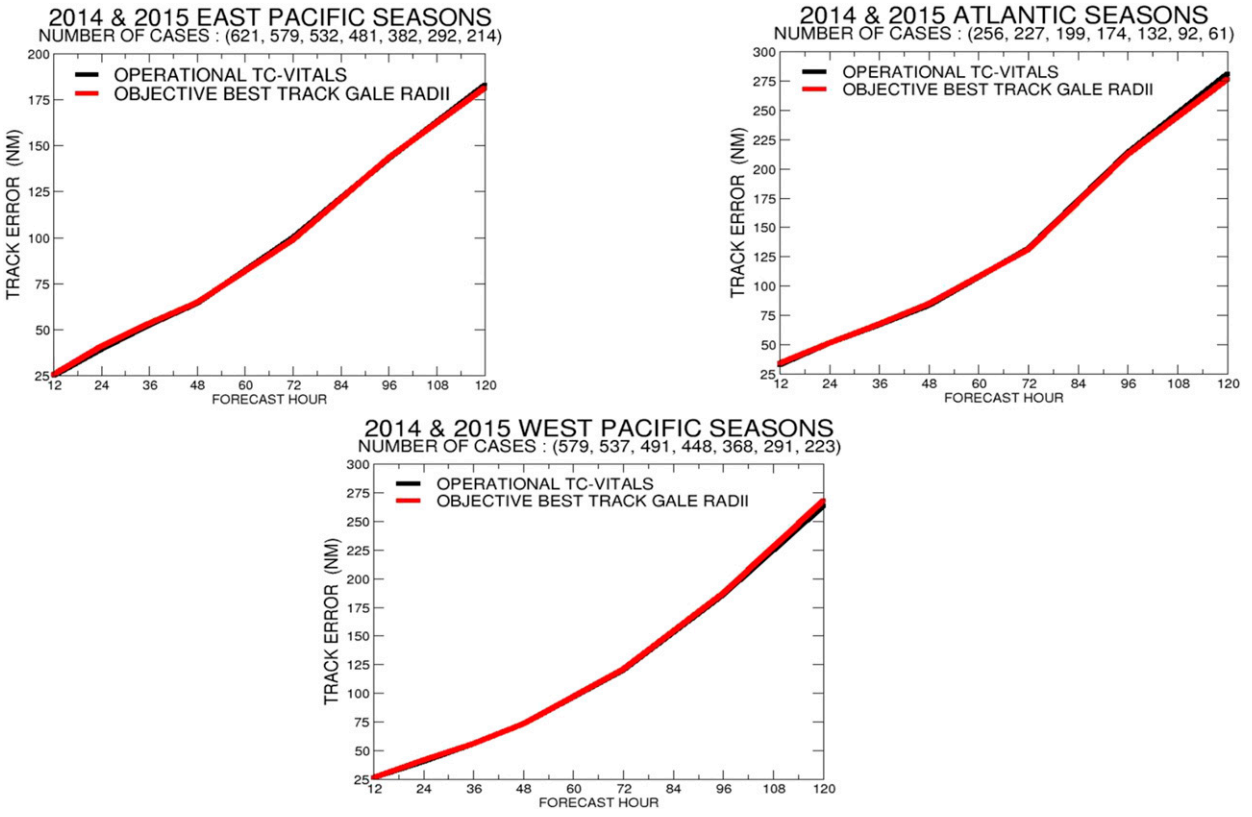

FIG. 6. Average track forecast error (n mi) for all forecasts run using gale wind radii from the operational TC vitals (black) and the OBTK (red) for the (top left) eastern Pacific, (top right) Atlantic, and (bottom) western Pacific for the combined 2014–15 seasons. The numbers of cases at forecast hours 12, 24, 36, 48, 72, 96, and 120 are indicated.

example, in the east Pacific, 12 of the 29 storms during the two seasons (40% of the sample) intensified more than 40 kt in 24 h. In the west Pacific, 9 of the 27 (33%) underwent intensification that exceeded 50 kt in 24 h. We refer to these subsets as extreme RI cases. Statistics were compiled for these sets of cases in both the east and west Pacific to better quantify the impact of the OBTK on the prediction of extreme RI events. Slightly different thresholds were chosen for these two basins to focus on a subset of storms that contained approximately the top one-third of the most rapidly intensifying TCs. The average intensity forecast errors and biases (Fig. 10) and PDF plots (Fig. 11) are shown just for this subset of cases, with the percent changes at all lead times and statistical significance summarized in Table 5. The experiment using the OBTK gale force wind radii had reduced average intensity errors in the 24–48-h forecast lead times relative to runs using the operational TC vitals, with maximum error reductions in the 1–2-day lead times of 14% and 17% in the east and west Pacific, respectively. These results were statistically significant at over 90% for all forecast lead times from 12 to 72 h (Table 5), with statistical significance exceeding 99% for forecast lead times from 12 to 36 h. Also note the large reduction of nearly 75% in the negative intensity bias in the west Pacific in the 12–72-h forecast time period (Fig. 10, bottom right) using gale force wind radii from OBTK, with a reduction in the negative bias of about 25% for the east Pacific. Similarly, a slightly larger decrease in the occurrence of errors is seen in the tail on the negative side of the PDF (Fig. 11), particularly in the number of cases with errors from −80 to −40 kt, clearly indicating improved forecasting of extreme RI events, as suggested in the earlier case studies (e.g., Typhoons Soudelor, Neoguri, and Nuri, as well as Hurricane Joaquin); however, a slightly larger positive bias in the west Pacific for the PDF is seen in cases where OBTK radii were used. Cursory examination of these cases suggests that although these RI events were better predicted, there was a tendency for some of these intense storms to not decay quickly enough, particularly during the rapid weakening phase following the time of maximum intensity. One possible contributing factor could be that the larger storm size is more resilient to shear reducing the rate of decay. This warrants further investigation but the primary focus of this present study is on the

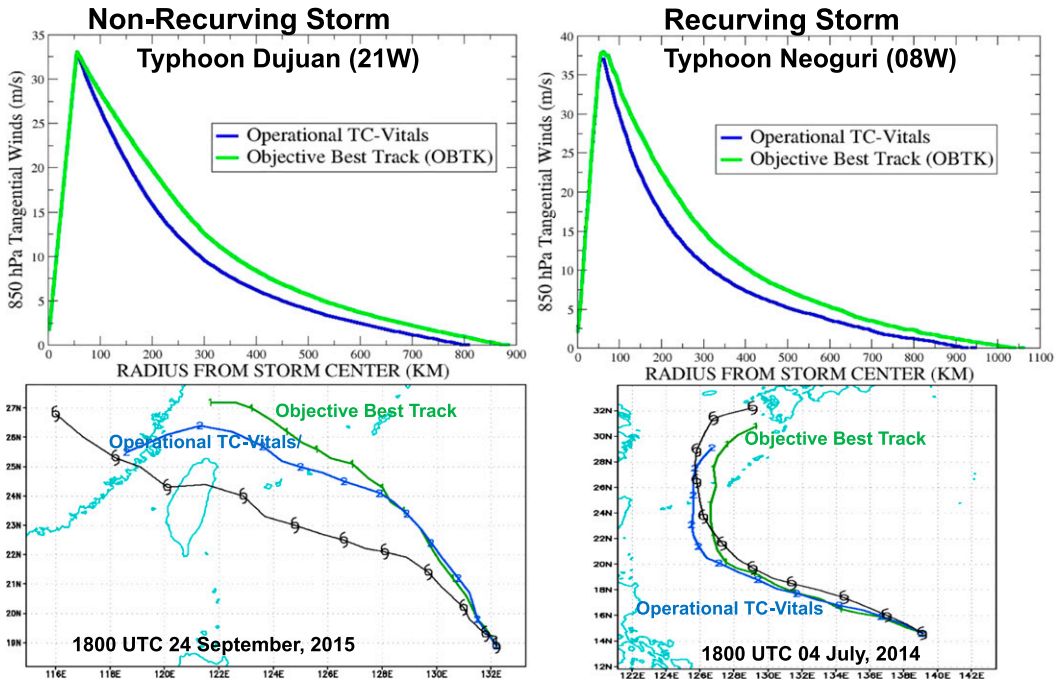

FIG. 7. Initial radial distribution of the (top) 850-hPa tangential wind and (bottom) forecast storm tracks using gale wind radii from the operational TC vitals (blue) and the OBTK (green), for (left) Typhoon Dujuan (21W) initialized at 1800 UTC 24 Sep 2015 and (right) Typhoon Neoguri (08W) initialized at 1800 UTC 4 Jul 2014.

impact of the prediction of RI events using the OBTK specification of storm size to initialize the storm vortex.

To better focus on the period during which RI was occurring, the average intensity errors for these RI cases were computed for only the forecast times up to and including maximum intensity (Fig. 12). Although the number of verifying cases was small, the improvement in the intensity predictions for periods of RI was large. The average intensity forecast error in the 1–3-day lead time for the west Pacific (Fig. 12) was reduced over 20% (from 24 to 19 kt) and the average negative bias decreased 40% (from −15 to −9 kt). In the east Pacific the error reductions averaged about 17% (from 31 to 27 kt; Fig. 12, left panels) and the negative bias decreased

TABLE 3. List of storms where the difference in the 5-day forecast error exceeded 10% between the operational TC vitals and the OBTK. Included is the basin, change in 5-day track error (%), whether the storm recurved or was nonrecurving, and the difference in the initial 34-kt radii using the OBTK (%).

Storm	Basin	Change in 5-day track error (%)	Recurve/nonrecurving	Change in initial 34-kt radii (%)
Norbert (14E; 2014)	East Pacific	+21	Nonrecurving	+9
Odile (15E; 2014)	East Pacific	+11	Nonrecurving	+3
Polo (17E; 2014)	East Pacific	+18	Nonrecurving	+10
Nora (18E; 2015)	East Pacific	+14	Nonrecurving	+45
Phanfone (18W; 2014)	West Pacific	+28	Nonrecurving	+29
Krovanh (20W; 2015)	West Pacific	+12	Recurving	+16
Dujuan (21W; 2015)	West Pacific	+33	Nonrecurving	+12
Danny (04L; 2014)	Atlantic	+33	Nonrecurving	+15
Blanca (02E; 2015)	East Pacific	−16	Nonrecurving	+4
Dolores (05E; 2015)	East Pacific	−34	Nonrecurving	+25
Cristobal (04L; 2015)	Atlantic	−33	Recurving	+2
Edouard (06L; 2014)	Atlantic	−17	Recurving	+7
Nuri (20W; 2014)	West Pacific	−26	Recurving	+22
Neoguri(08W; 2014)	West Pacific	−25	Recurving	+29
Atsani (17W; 2015)	West Pacific	−12	Recurving	+20
Avg change		+0.2		+15

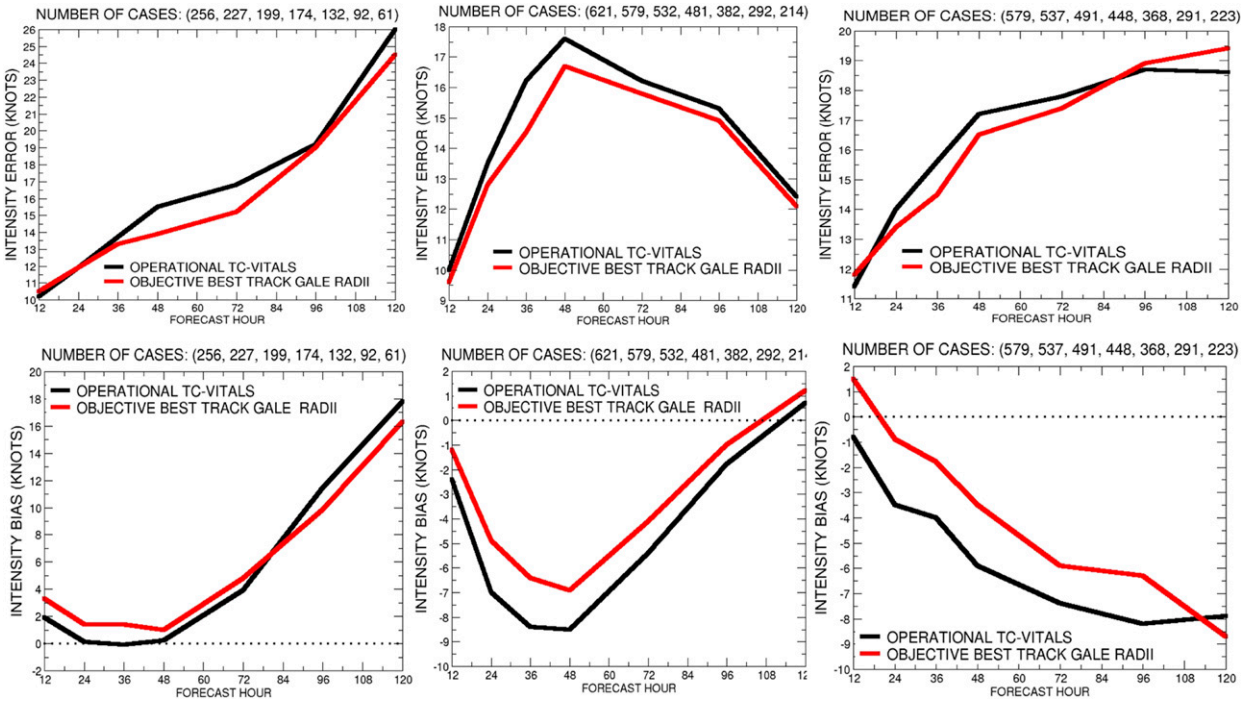

FIG. 8. (top) Average intensity forecast errors (kt) and (bottom) intensity bias (kt) for all forecasts run using gale wind radii from the operational TC vitals (black) and the OBTK (red) for the (left) Atlantic, (center) east Pacific, and (right) west Pacific for the combined 2014–15 seasons. The numbers of cases at forecast hours 12, 24, 36, 48, 72, 96, and 120 are indicated.

15%. Although the number of verifying forecasts is small, this again suggests that a much improved prediction of extreme RI was achieved for the GFDL model when the TC structure was initialized using the OBTK radii.

Finally, as shown previously, in the west Pacific, unlike in the Atlantic and the east Pacific, the OBTK method exhibited average gale force wind radii that were systematically larger (27%) than JTWC's operational TC vitals (Table 1). A supplemental set of forecasts was run in this basin, performed by increasing the operational TC vitals wind radii by 25% and by using the sample of storms in the west Pacific sample that underwent 50 kt $(24\,\text{h})^{-1}$ RI. The question that was addressed during this experiment was whether the improved prediction of RI could be achieved by simply correcting for this systematic negative bias. Results for the subset (hereafter, P25) of forecasts are shown in Fig. 13. In the 1–2-day forecast period, where the largest improvement was found using the OBTK gale force wind radii for this set of extreme RI cases, adding a 25% bias correction to the operational TC vitals file did not reduce the large negative intensity forecast biases nor the intensity forecast errors as much as forecasts that used the OBTK wind radii. In fact, the intensity forecast errors in that 1–2-day lead time were only marginally reduced from those with the control runs using the operational TC vitals. The PDFs and CDFs (Fig. 13, right panels) show that the small number of forecasts with negative biases in excess of 70 kt was removed in the P25 experiment with the increased radii, but the number of forecasts with a negative bias of 30–60 kt was similar to the number in the control experiment. Also, the P25 and OBTK experiments increased the number of forecasts with positive bias, which again appears to be resulting from too slow

TABLE 4. Percent change in forecast intensity error and p value of the statistical significance using the OBTK radii vs the operational TC vitals, for all cases run in the Atlantic, east Pacific, and west Pacific, using a one-tailed Student's t test. Asterisks indicate forecast lead times where the changes did not result in p values for statistical significance of at least 90%. Boldface font is used to indicate p values that exceed 95%.

	% change/p value		
Forecast hour	Atlantic	East Pacific	West Pacific
12	2%/*	−5%/**98%**	3%/*
24	0%/*	−5%/**100%**	−4%/94%
36	−3%/*	−10%/**100%**	−7%/**100%**
48	−10%/**99%**	−5%/**100%**	−4%/**96%**
72	−10%/**99%**	−3%/91%	−2%/*
96	−1%/*	−3%/*	1%/*
120	−6%/*	−2%/*	4%/*

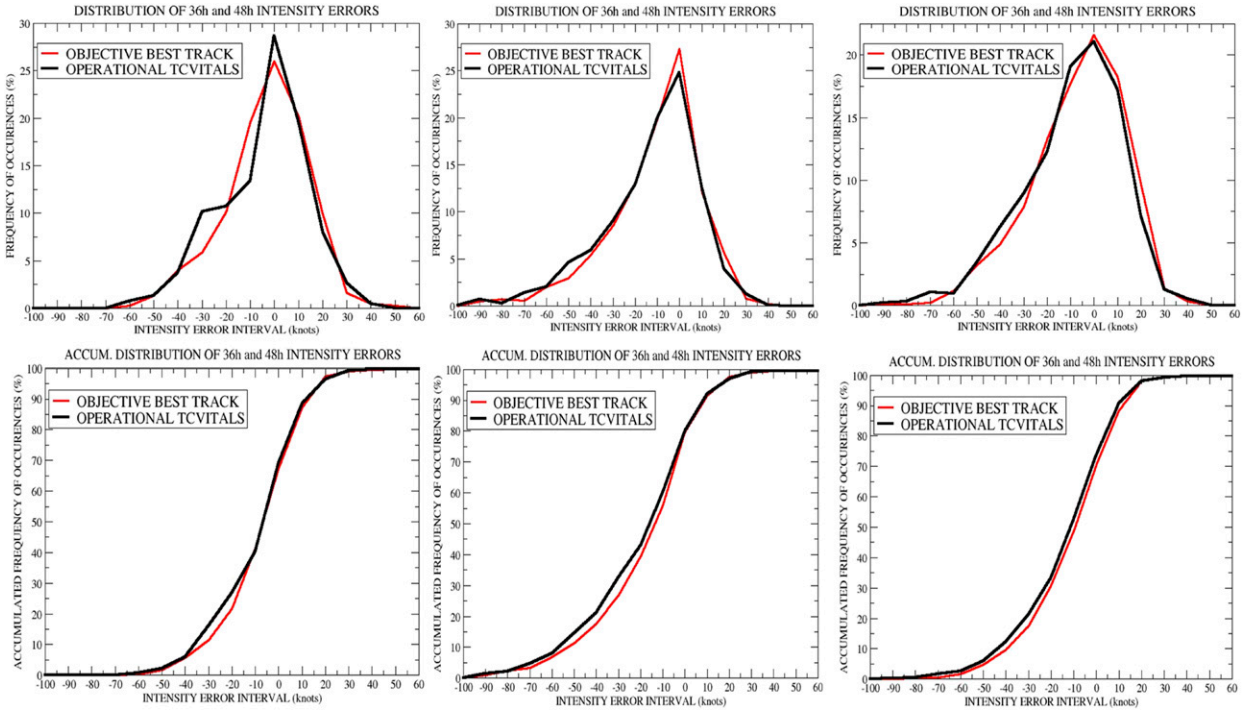

FIG. 9. (top) PDFs and (bottom) CDFs for the combined 36- and 48-h intensity forecast errors using gale wind radii from the operational TC vitals (black) and OBTK (red) for the (left) Atlantic, (center) east Pacific, and (right) west Pacific, for the combined 2014–15 seasons.

weakening after the period of RI, particularly for the most intense storms. Overall, results suggest that the amount of improvement in the prediction of RI in the west Pacific with the OBTK would not have been achieved by systematically increasing the gale wind radii, and that improved representation of an individual TC wind structure also contributed to reducing the intensity errors. This finding is also consistent with the improved intensity prediction shown in the other two basins. This is particularly true in the Atlantic, where TC vitals and the OBTK wind radii averages were nearly identical, but intensity forecasts were significantly improved when OBTK wind radii were used for the GFDL initialization. This also demonstrates the value of the OBTK methodology and the potential benefits that may be obtained from a more consistent and possibly more accurate specification of the storm size R_b and surface wind structure.

4. Discussion and summary

Previous studies have suggested that more accurate estimates of TC size and structure used to initialize NWP models could produce improved model forecasts. However, no systematic study to date has investigated this impact rigorously, that is, by using a sufficiently large number of cases over a multiyear sample, which is typically the criterion used in determining whether changes to operational guidance models are statistically significant and can lead to improved model performance (e.g., Zhang et al. 2016). An objective analysis (OBTK) was developed by Sampson et al. (2017) to estimate TC gale force wind radii in real time in the absence of scatterometer and aircraft data. Results from their study showed that the OBTK can, on average, produce storm structure estimates that are comparable to NHC real-time estimates in the Atlantic and east Pacific and are approximately 25% larger than real-time estimates from JTWC in the west Pacific. The OBTK also produces a smoother temporal evolution of the gale force wind radii.

The GFDL hurricane forecast system, operational for 22 years by the NWS and 21 years by the U.S. Navy (Bender et al. 2007), was an ideal candidate for evaluating the impact of the objective radii. The 2014 and 2015 hurricane/typhoon seasons were chosen (July–November) because of the availability of the 2016 version of the NWS GFS global model. The initial storm size R_b in the GFDL model used here is a function of the average radii of the estimated gale force winds, assuming conservation of angular momentum principles, and thus is very sensitive to the initial gale force wind radii. The impact of using the TC vitals–based (control) versus the OBTK-based (experiment) gale force wind radii

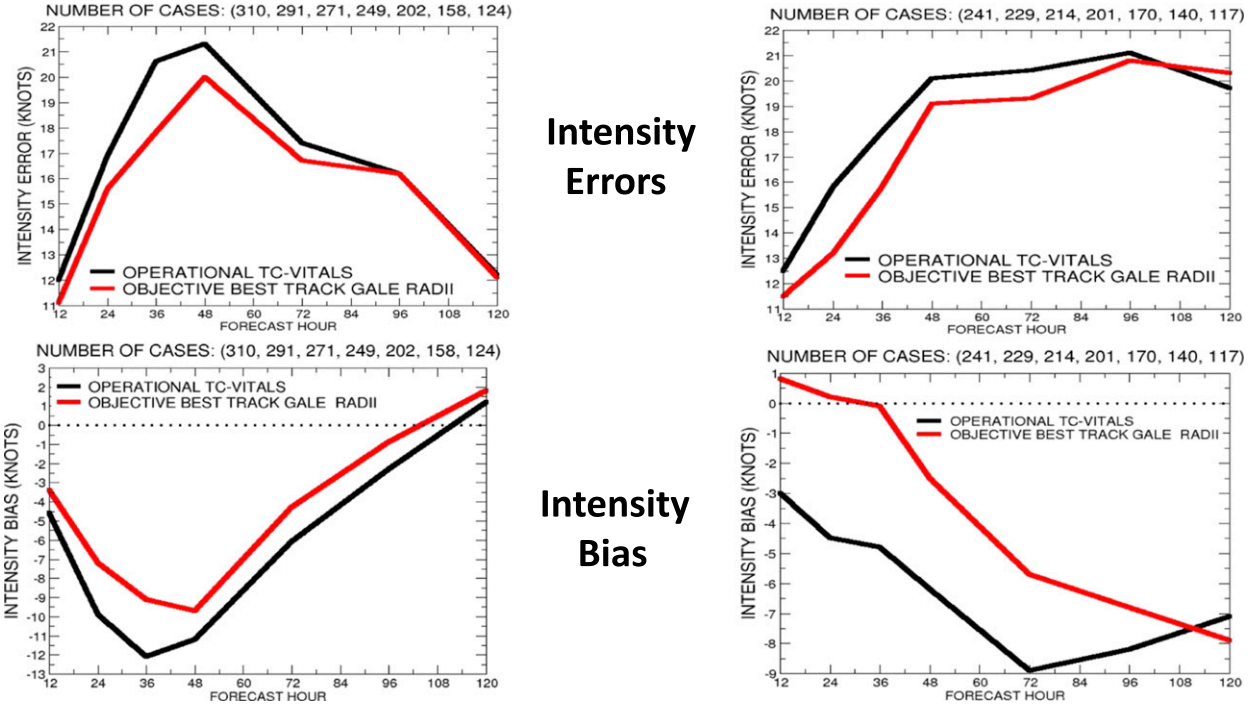

FIG. 10. (top) Average intensity forecast errors (kt) and (bottom) intensity forecast bias (kt) using the operational TC vitals (black) and the OBTK (red) for the (left) east and (right) west Pacific for those cases undergoing RI of 40 and 50 kt $(24\,h)^{-1}$, respectively, for the combined 2014–15 seasons. The numbers of cases at forecast hours 12, 24, 36, 48, 72, 96, and 120 are indicated.

for initialization on the GFDL TC forecasts was investigated using a 2-yr dataset and cases from three ocean basins (Atlantic, and east and west Pacific). These experiments produced 1529 forecasts.

Results indicate that the use of the OBTK had a neutral impact on the average track error in each of the three basins (e.g., improvements in only 51% of the forecasts at lead times of 2–5 days). Examination of individual cases found that of the TCs with differences in the 5-day track error exceeding 10% (~20% of the total sample), eight storms were significantly degraded, seven improved, and the average impact was neutral (0.2%). Most of the forecasts with reduced track errors in the OBTK experiment were associated with recurving storms while the largest degradation was for nonrecurving, west-moving storms where a significant slow bias (80 n mi at day 5) resulted. These cases were likely impacted by the intensity evolution of the forecasted storms as the control forecasts exhibited 2–3 times greater negative intensity biases compared to the forecasts initialized with the OBTK, indicative of a weaker system moving faster under the influence of the subtropical ridge. In the recurving forecasts, where the storms initialized using the OBTK were also significantly stronger, the reduced slow biases prior to and during recurvature were consistent with the upper-level interaction of deeper circulations with the westerlies. It is also possible that the beta drift was increased (i.e., larger TCs tend to drift north faster than smaller TCs), but the two effects are nearly impossible to separate.

The bulk of the analysis in this study, however, focused on the intensity forecasts where the average intensity forecasts were significantly improved in all three basins when using the modified gale force radii from the OBTK particularly in the critical 1–2-day time range. Although the average improvement was modest, averaging about 4%–10%, it was found that the improvement was considerably greater for storms undergoing RI, particularly during the onset of RI, where the 1–3-day intensity errors decreased over 20% in the west Pacific and about 17% in the east Pacific in the 1–3 day period leading up to the time of maximum intensity. For the 12 east Pacific storms in this sample that underwent RI of at least 40 kt in 24 h, the 36-h negative intensity bias decreased 25% from −12 to −9 kt. A large reduction in negative intensity basis was also achieved for the west Pacific, for the nine storms that experienced extreme RI events (50 kt or greater in 24 h), where the 1–3-day (negative) bias was reduced nearly 75%. This result is particularly encouraging in the east Pacific, where a large negative bias has been a persistent problem in both the GFDL and HWRF operational hurricane

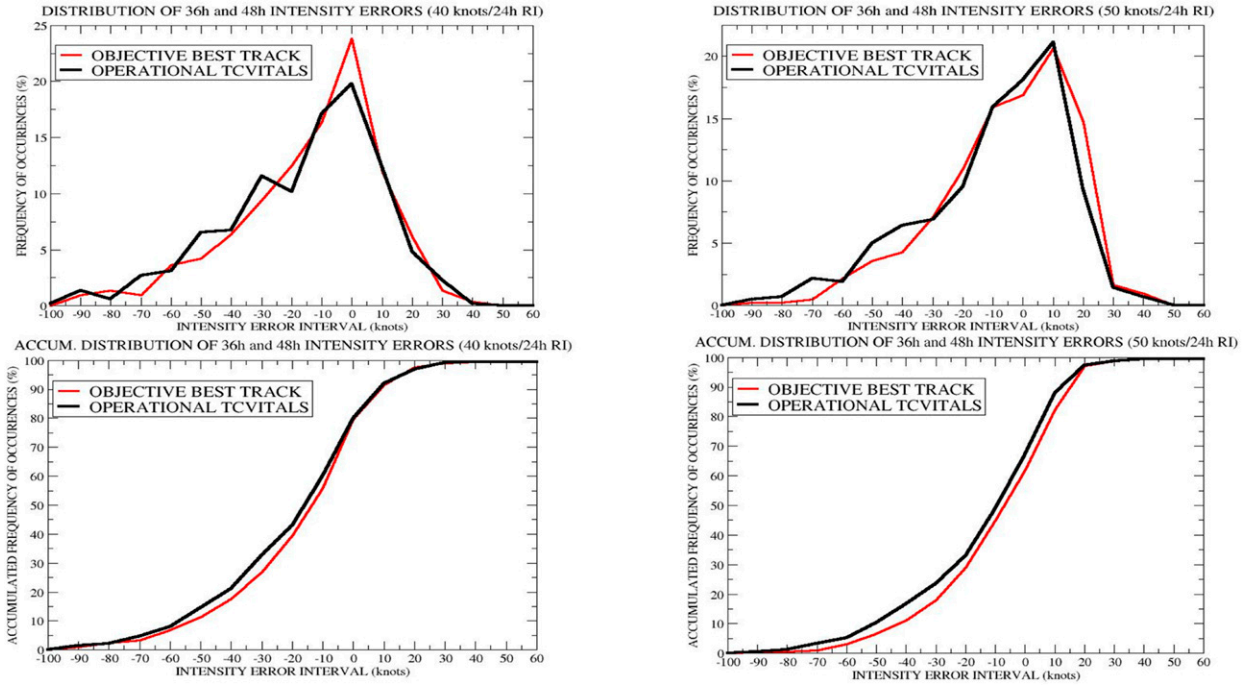

FIG. 11. (top) PDFs and (bottom) CDFs of combined 36- and 48-h intensity forecast errors using gale wind radii from the operational TC vitals (black) and the OBTK (red) for the (left) east and (right) west Pacific for those cases undergoing RI of 40 and 50 kt $(24\,h)^{-1}$, respectively, for the combined 2014–15 seasons.

models (Cangialosi and Franklin 2015, 2016). Since the OBTK provides gale force wind radii estimates that are superior to other techniques, particularly in the west Pacific (see Sampson et al. 2017, their Fig. 2), these results suggest that proper specification of the gale force wind radii and the storm size may be critical to achieving a more reliable forecast of RI using high-resolution regional models. These results, based solely on the GFDL hurricane model, are nonetheless very encouraging.

Considering the abovementioned results, it should be pointed out that when changes to operational models were tested prior to previous model upgrades, it is common for the performance for some storms and synoptic situations to be significantly improved and others degraded. The criterion followed for operational implementation is that the overall average impact must be positive for a large enough sample size so that statistical significance can be demonstrated. Since biases can be significantly different with other models, it is possible that the impacts of OBTK-based wind radii on the performance of track and intensity forecasts may be different for other modeling systems as a result of model errors, biases, and how they use the gale force wind radii for initialization. This study, however, highlights the need for testing model sensitivities to the gale force wind radii and other TC vitals–based information in other modeling systems. Such evaluation would also allow for more definitive conclusions to be made concerning model sensitivities to the initial specification of the wind radii.

TABLE 5. As in Table 4, but only for the storms that underwent RI of at least 40 kt in the east Pacific and 50 kt in the west Pacific.

	% change/p value	
Forecast hour	East Pacific [40 kt $(24\,h)^{-1}$]	West Pacific [50 kt $(24\,h)^{-1}$]
12	−8%/**100%**	−7%/**100%**
24	−8%/**100%**	−17%/**100%**
36	−14%/**100%**	−12%/**100%**
48	−6%/**100%**	−5%/92%
72	−4%/90%	−5%/93%
96	0%/*	−2%/*
120	−1%/*	−3%/*

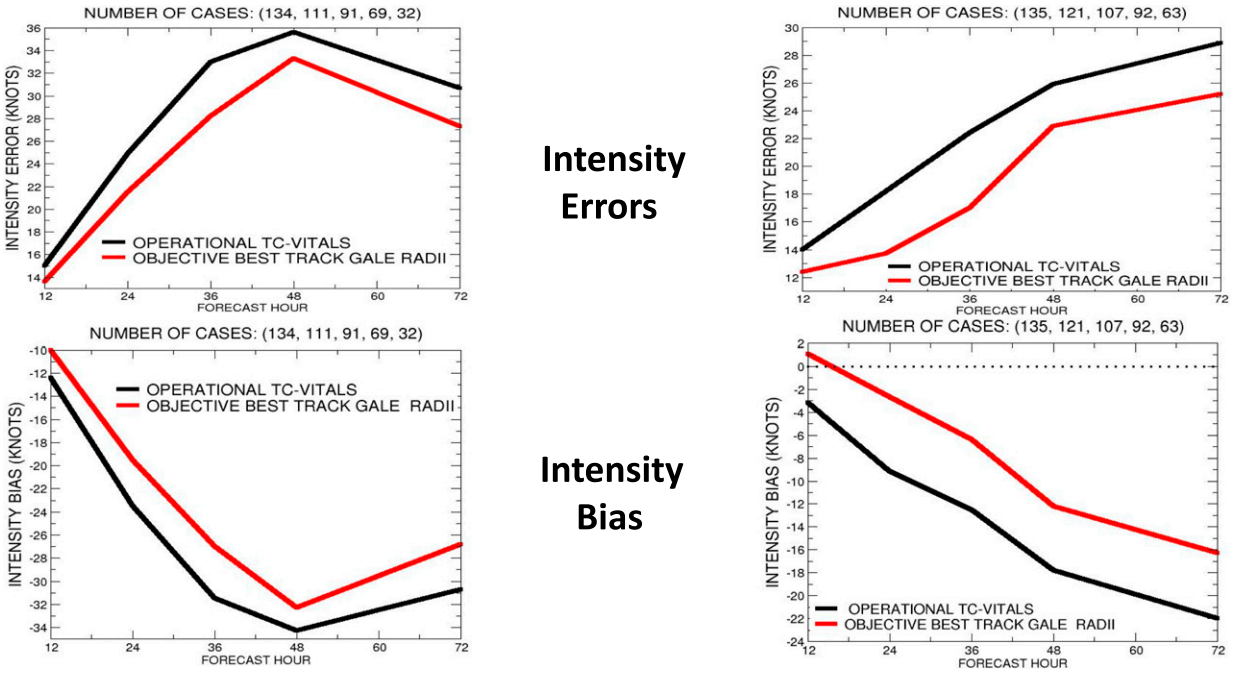

FIG. 12. (top) Average intensity forecast errors (kt) and (bottom) intensity forecast bias (kt) using the operational TC vitals (black) and the OBTK (red) for the (left) eastern and (right) western Pacific for those cases prior to reaching maximum intensity and that underwent RI of 40 and 50 kt (24 h)$^{-1}$, respectively, for the combined 2014–15 seasons. The numbers of cases at forecast hours 12, 24, 36, 48, and 72 are also shown.

Importantly, it should be pointed out that this study focused on the impact of the accurate specification of the storm size and radial extent of the gale force wind radii on the forecast of TC track and intensity from NWP models. Significant improvement in the forecast of storm intensity and RI may also be achieved with better initialization of the inner-core structure of the tropical cyclone. This is a topic that will become increasingly important as regional hurricane models obtain higher resolution and better data assimilation (DA) methods are developed, which will allow high quality data from aircraft observations, radar, and other remote platforms to be properly ingested into the storm core. This study suggests that improved initialization likely will have a significant impact on developing more successful short-term predictions, including those of RI events. Undoubtedly, DA of satellite radiances will eventually become a vital part of the vortex initialization. Since this is presently not the case, all operational hurricane modeling systems use information from the TC vitals files to improve the presentation of the initial vortex (e.g., GFDL, HWRF, COAMPS-TC). This important topic is beyond the scope of this present work and will be a topic for future research.

For the present, this study has demonstrated that improving the TC vitals should lead to better initialization and thus improved prediction, until DA systems can properly initialize the hurricane vortex, and these systems can be run efficiently to be practical for real-time NWP hurricane forecasting applications. The authors also hope that this study, by showing the benefits of quality TC structure estimates on NWP intensity forecasts, will 1) reinforce the need for highly accurate operational TC structure estimates and 2) justify the time needed in the forecast cycle to make such estimates. It is also hoped that this study will help to quantify the potential benefits (beyond saving forecasters time) that the OBTK may have in improving the estimation of the gale force wind radii, particularly as this technique is improved and refined in future upgrades. Finally, it is the authors' hope that the robustness of the results and conclusions presented here will be evaluated with other models and modeling systems.

Acknowledgments. The authors wish to thank Andrew Hazelton, Kun Gao, and Kieran Bhatia of the Princeton University AOS Program for their reviews and comments on an earlier version of the manuscript. The continued support of tropical cyclone research provided by the Office of Naval Research is sincerely appreciated. We are grateful for the Hurricane Forecast Improvement Project, which provided computer resource on the

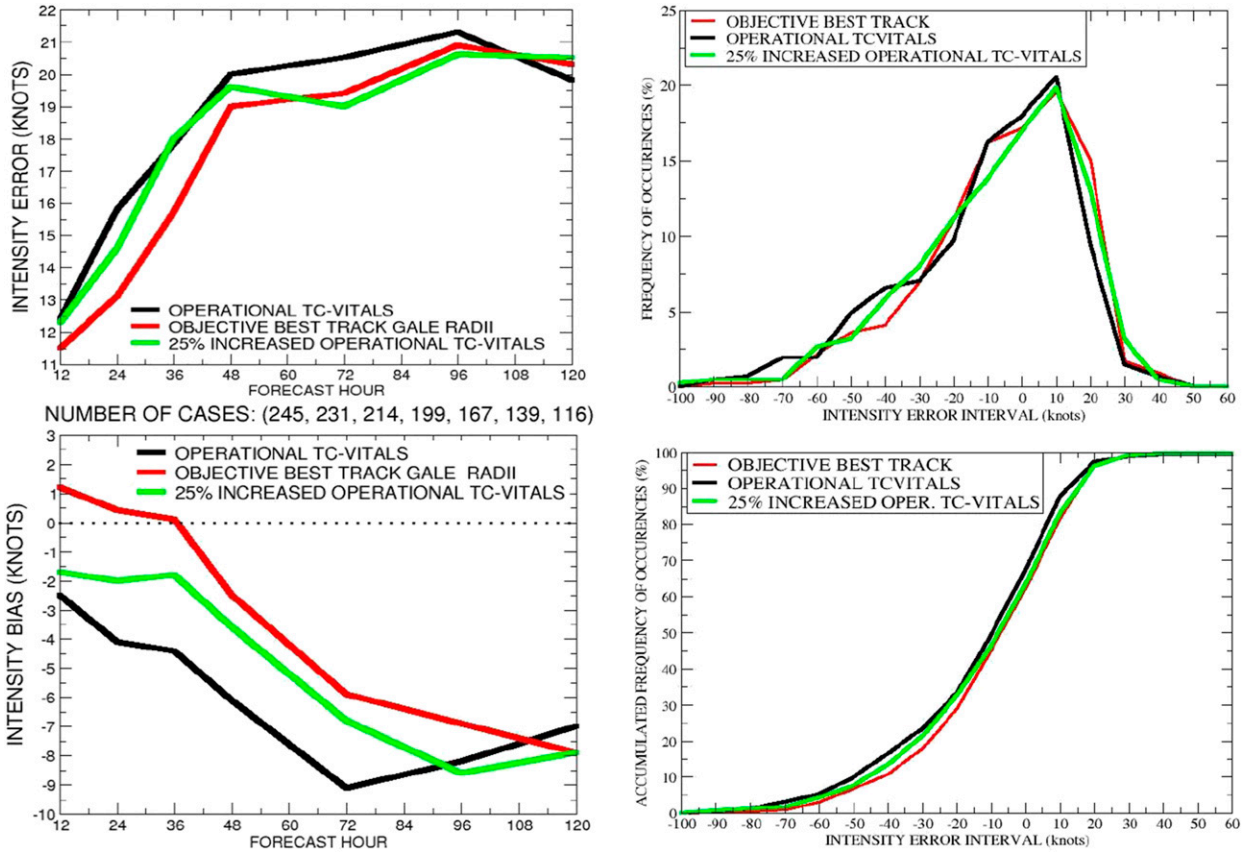

FIG. 13. (top left) Average intensity errors (kt), (bottom left) intensity bias (kt), (top right) PDFs and (bottom right) CDFs of the combined 36- and 48-h intensity errors for the western Pacific, using the operational TC vitals (black), the OBTK (red), and a supplemental experiment (P25) using the operational TC vitals (green) and 25% increased gale radii. The numbers of cases at forecast hours 12, 24, 36, 48, 72, 96, and 120 h are indicated.

Jet supercomputer facility, where these simulations were made. We also thank three anonymous reviewers whose very insightful comments significantly improved the revised version of this manuscript. Finally, we are especially grateful to V. Ramaswamy, director of GFDL, for his continued support of the hurricane project at GFDL. The views, opinions, and findings contained in this report are those of the authors and should not be construed as an official National Oceanic and Atmospheric Administration or U.S. government position, policy, or decision.

REFERENCES

Anthes, R. A., and J. E. Hoke, 1975: The effect of horizontal divergence and latitudinal variation of the Coriolis parameter on the drift of a model hurricane. *Mon. Wea. Rev.*, **103**, 757–763, doi:10.1175/1520-0493(1975)103<0757:TEOHDA>2.0.CO;2.

Bender, M. A., I. Ginis, R. Tuleya, B. Thomas, and T. Marchok, 2007: The operational GFDL coupled hurricane–ocean prediction system and a summary of its performance. *Mon. Wea. Rev.*, **135**, 3965–3989, doi:10.1175/2007MWR2032.1.

——, M. J. Morin, K. Emanuel, J. A. Knaff, C. Sampson, I. Ginis, and B. Thomas, 2016: Impact of storm structure and the environmental conditions in the rapid intensification of Hurricanes Katrina and Patricia. *32nd Conf. on Hurricanes and Tropical Meteorology*, San Juan, PR, Amer. Meteor. Soc. [Available online at https://ams.confex.com/ams/32Hurr/webprogram/Paper293687.html.]

Cangialosi, J., and J. Franklin, 2015: 2014 National Hurricane Center forecast verification report. National Hurricane Center, 82 pp. [Available online at http://www.nhc.noaa.gov/verification/pdfs/Verification_2014.pdf.]

——, and ——, 2016: National Hurricane Center forecast verification report: 2015 hurricane season. National Hurricane Center, 69 pp. [Available online at http://www.nhc.noaa.gov/verification/pdfs/Verification_2015.pdf.]

Carr, L., and R. Elsberry, 1997: Models of tropical cyclone wind distribution and beta-effect propagation for application to tropical cyclone track forecasting. *Mon. Wea. Rev.*, **125**, 3190–3209, doi:10.1175/1520-0493(1997)125<3190:MOTCWD>2.0.CO;2.

DeMaria, M., 1985: Tropical cyclone motion in a nondivergent barotropic model. *Mon. Wea. Rev.*, **113**, 1199–1210, doi:10.1175/1520-0493(1985)113<1199:TCMIAN>2.0.CO;2.

——, J. A. Knaff, R. Knabb, C. Lauer, C. R. Sampson, and R. T. DeMaria, 2009: A new method for estimating tropical cyclone

wind speed probabilities. *Wea. Forecasting*, **24**, 1573–1591, doi:10.1175/2009WAF2222286.1.

——, and Coauthors, 2013: Improvements to the operational tropical cyclone wind speed probability model. *Wea. Forecasting*, **28**, 586–602, doi:10.1175/WAF-D-12-00116.1.

Demuth, J., M. DeMaria, J. A. Knaff, and T. H. Vonder Haar, 2004: Validation of an Advanced Microwave Sounder Unit (AMSU) tropical cyclone intensity and size estimation algorithm. *J. Appl. Meteor. Climatol.*, **43**, 282–296, doi:10.1175/1520-0450(2004)043<0282:EOAMSU>2.0.CO;2.

——, ——, and ——, 2006: Improvement of Advanced Microwave Sounding Unit tropical cyclone intensity and size estimation algorithms. *J. Appl. Meteor. Climatol.*, **45**, 1573–1581, doi:10.1175/JAM2429.1.

Fiorino, M., and R. L. Elsberry, 1989: Some aspects of vortex structure related to tropical cyclone motion. *J. Atmos. Sci.*, **46**, 975–990, doi:10.1175/1520-0469(1989)046<0975:SAOVSR>2.0.CO;2.

Hogan, T. F., and Coauthors, 2014: The Navy Global Environmental Model. *Oceanography*, **27** (3), 116–125, doi:10.5670/oceanog.2014.73.

Holland, G., 1984: Tropical cyclone motion: A comparison of theory and observation. *J. Atmos. Sci.*, **41**, 68–75, doi:10.1175/1520-0469(1984)041<0068:TCMACO>2.0.CO;2.

Holmlund, K., C. Velden, and M. Rohn, 2001: Enhanced automated quality control applied to high-density satellite-derived winds. *Mon. Wea. Rev.*, **129**, 517–529, doi:10.1175/1520-0493(2001)129<0517:EAQCAT>2.0.CO;2.

Jones, W. L., W. L. Grantham, L. C. Schroeder, J. W. Johnson, C. T. Swift, and J. L. Mitchell, 1975: Microwave scattering from the ocean surface. *IEEE Trans. Microwave Theory Tech.*, **23**, 1053–1058, doi:10.1109/TMTT.1975.1128742.

Kaplan, J., and M. DeMaria, 2003: Large-scale characteristics of rapidly intensifying tropical cyclones in the North Atlantic basin. *Wea. Forecasting*, **18**, 1093–1108, doi:10.1175/1520-0434(2003)018<1093:LCORIT>2.0.CO;2.

Knaff, J. A., and B. A. Harper, 2010: Tropical cyclone surface wind structure and wind-pressure relationships. *Proc. WMO Int. Workshop on Tropical Cyclones—VII*, La Reunion, France, WMO, KN1. [Available online at http://www.wmo.int/pages/prog/arep/wwrp/tmr/otherfileformats/documents/KN1.pdf.]

——, and C. R. Sampson, 2015: After a decade are Atlantic tropical cyclone gale force wind radii forecasts now skillful? *Wea. Forecasting*, **30**, 702–709, doi:10.1175/WAF-D-14-00149.1.

——, M. DeMaria, D. A. Molenar, C. R. Sampson, and M. G. Seybold, 2011: An automated, objective, multisatellite platform tropical cyclone surface wind analysis. *J. Appl. Meteor. Climatol.*, **50**, 2149–2166, doi:10.1175/2011JAMC2673.1.

——, C. J. Slocum, K. D. Musgrave, C. R. Sampson, and B. R. Strahl, 2016: Using routinely available information to estimate tropical cyclone wind structure. *Mon. Wea. Rev.*, **144**, 1233–1247, doi:10.1175/MWR-D-15-0267.1.

Kunii, M., 2015: Assimilation of tropical cyclone track and wind radius data with an ensemble Kalman filter. *Wea. Forecasting*, **30**, 1050–1063, doi:10.1175/WAF-D-14-00088.1.

Kurihara, Y., M. A. Bender, and R. J. Ross, 1993: An initialization scheme of hurricane models by vortex specification. *Mon. Wea. Rev.*, **121**, 2030–2045, doi:10.1175/1520-0493(1993)121<2030:AISOHM>2.0.CO;2.

——, ——, R. E. Tuleya, and R. J. Ross, 1995: Improvements in the GFDL hurricane prediction system. *Mon. Wea. Rev.*, **123**, 2791–2801, doi:10.1175/1520-0493(1995)123<2791:IITGHP>2.0.CO;2.

Landsea, C. W., and J. L. Franklin, 2013: Atlantic hurricane database uncertainty and presentation of a new database format. *Mon. Wea. Rev.*, **141**, 3576–3592, doi:10.1175/MWR-D-12-00254.1.

Madala, R. V., and A. A. Piacsek, 1975: Numerical simulation of asymmetric hurricanes on a B-plane with vertical shear. *Tellus*, **27**, 453–468, doi:10.3402/tellusa.v27i5.10172.

Marchok, T., M. Morin, and M. Bender, 2012: Evaluation of a GFDL hurricane model ensemble forecast system. *30th Conf. on Hurricanes and Tropical Meteorology*, Vedra Beach, FL, Amer. Meteor. Soc., 13A.3. [Available online at https://ams.confex.com/ams/30Hurricane/webprogram/Paper206200.html.]

Montgomery, M., and R. Smith, 2014: Paradigms for tropical cyclone intensification. *Aust. Meteor. Oceanogr. J.*, **64**, 37–66, doi:10.22499/2.6401.005.

Neumann, C. J., M. B. Lawrence, and E. L. Caso, 1977: Monte Carlo significance testing as applied to statistical tropical cyclone models. *J. Appl. Meteor.*, **16**, 1165–1174, doi:10.1175/1520-0450(1977)016<1165:MCSTAA>2.0.CO;2.

Sampson, C. R., and A. J. Schrader, 2000: The Automated Tropical Cyclone Forecasting System (version 3.2). *Bull. Amer. Meteor. Soc.*, **81**, 1231–1240, doi:10.1175/1520-0477(2000)081<1231:TATCFS>2.3.CO;2.

——, P. A. Wittman, and H. L. Tolman, 2010: Consistent tropical cyclone wind and wave forecasts for the U.S. Navy. *Wea. Forecasting*, **25**, 1293–1306, doi:10.1175/2010WAF2222376.1.

——, and Coauthors, 2012: Objective guidance for use in setting tropical cyclone conditions of readiness. *Wea. Forecasting*, **27**, 1052–1060, doi:10.1175/WAF-D-12-00008.1.

——, E. Fukada, J. A. Knaff, B. R. Strahl, M. J. Brennan, and T. Marchok, 2017: Tropical cyclone gale wind radii estimates for the western North Pacific. *Wea. Forecasting*, **32**, 1029–1040, doi:10.1175/WAF-D-16-0196.1.

Tallapragada, V., and Coauthors, 2014: Hurricane Weather Research and Forecasting (HWRF) Model: 2014 scientific documentation. Developmental Testbed Center, 105 pp. [Available online at http://www.dtcenter.org/HurrWRF/users/docs/scientific_documents/HWRFv3.6a_ScientificDoc.pdf.]

Velden, C., and Coauthors, 2005: Recent innovations in deriving tropospheric winds from meteorological satellites. *Bull. Amer. Meteor. Soc.*, **86**, 205–223, doi:10.1175/BAMS-86-2-205.

Wu, C.-C., G.-Y. Lien, J.-H. Chen, and F. Zhang, 2010: Assimilation of tropical cyclone track and structure based on the ensemble Kalman filter (EnKF). *J. Atmos. Sci.*, **67**, 3806–3822, doi:10.1175/2010JAS3444.1.

Zhang, X., S. G. Gopalakrishnan, S. Trahan, T. S. Quirino, Q. Liu, Z. Zhang, G. Alaka, and V. Tallapragada, 2016: Representing multiscale interactions in the Hurricane Weather Research and Forecasting modeling system: Design of multiple sets of movable multi-level nesting and the basin-scale HWRF forecast application. *Wea. Forecasting*, **31**, 2019–2034, doi:10.1175/WAF-D-16-0087.1.